

Fig. 4 Corridor width as a function of entry velocity for 7-g limit, a) low-energy, 500-km circular orbit and b) high-energy, 1-sol orbit.

ties between 6.5–8.0 km/s are more attractive for minimizing the vehicle  $L/D$ . For conjunction-class missions in general, an aerocapture vehicle with an  $L/D$  of 0.22–0.28 will achieve high-energy orbits for entry velocities between 6.5–8.0 km/s.

## References

- <sup>1</sup>Chapman, D. R., "An Analysis of the Corridor and Guidance Requirements for Supercircular Entry Into Planetary Atmospheres," NASA TR R-55, 1960.
- <sup>2</sup>Cruz, M. I., "The Aerocapture Vehicle Mission Design Concept—Aerodynamically Controlled Capture of Payload into Mars Orbit," AIAA Paper 79-0893, May 1979.
- <sup>3</sup>Tauber, M. E., Bowles, J. V., and Yang, L., "The Use of Atmospheric Braking During Mars Missions," *Journal of Spacecraft and Rockets*, Vol. 27, No. 5, 1990, pp. 514–521.
- <sup>4</sup>Braun, R. D., Powell, R. W., and Hartung, L. C., "Effect of Interplanetary Trajectory Options on a Manned Mars Aerobrake Configuration," NASA TP-3019, Aug. 1990.
- <sup>5</sup>Lyne, J. E., "The Effect of Parking Orbit Selection on Manned Aerocapture at Mars," AAS/AIAA Paper 92-103, Feb. 1992.
- <sup>6</sup>Duke, M. B., Keaton, P., Weaver, D., Roberts, B., Briggs, G., and Huber, W., "Mission Objectives and Comparison of Strategies for Mars Exploration," AIAA Paper 93-0956, Feb. 1993.
- <sup>7</sup>Desai, P. N., and Braun, R. D., "Mars Parking Orbit Selection," *The Journal of Astronautical Sciences*, Vol. 39, No. 4, 1991, pp. 447–467.

<sup>8</sup>Lyne, J. E., "Physiologically Constrained Aerocapture for Manned Mars Missions," NASA TM-103954, Aug. 1992.

<sup>9</sup>Tauber, M., Chargin, M., Henline, W., Chiu, A., Yang, L., Hamm, K. R., Jr., and Miura, H., "Aerobrake Design Studies for Manned Mars Missions," AIAA Paper 91-1344, June 1991.

## Wing Effects on Missile Asymmetric Vortex Behavior

R. M. Howard,\* M. H. Lung,† J. J. Viniotis,‡  
D. A. Johnson,§ and J. A. Pinaire‡  
Naval Postgraduate School,  
Monterey, California 93943

### Introduction

THE introduction of a vertical launch capability for ships carrying surface-to-air missiles represents a major advancement in weapon system technology. But a characteristic of vertically launched missiles is their inability to point at the target intercept point prior to launch. Because the missile cannot rely on the fire-control radar beam to guide it into its initial intercept trajectory, it must be maneuvered into this flight path. The requirement for certain trajectories can place high angle-of-attack demands of up to 50 deg on the missile.<sup>1</sup>

The existence of an induced side force on slender bodies caused by the formation of asymmetric vortices at high angles of attack has been characterized by numerous investigators.<sup>2–4</sup> Unpredictable side forces may be generated under certain flow conditions for the vertically launched missile, posing a potential threat to flight stability. In 1987 a flight test was performed on the Vertical Launch Anti-Submarine Rocket (ASROC) (VLA) standoff weapon, requiring a hard pushover maneuver to a 70-deg angle of attack. During the maneuver, control of the missile was lost because of yawing moments 150% greater than those measured in wind-tunnel tests. A short time before departure, the nose cap tip became unseated; about 0.25 seconds later, the tip resealed itself, but the yawing moment continued, and control could not be regained. The incident was attributed to asymmetric vortex shedding.<sup>5</sup>

Although many studies have been performed considering slender bodies at high angles of attack, much less work has been done treating the influence of realistic wing planforms on

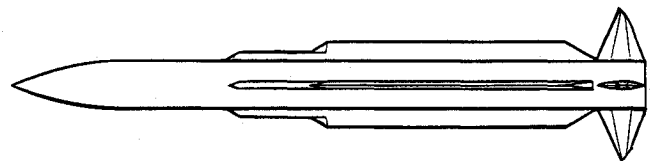


Fig. 1 Vertical launch surface-to-air missile model.

Received June 22, 1990; revision received July 15, 1991; accepted for publication Dec. 1, 1993. This paper is declared a work of the U.S. Government and is not subject to copyright protection in the United States.

\*Associate Professor, Department of Aeronautics and Astronautics, Senior Member AIAA.

†Graduate Student, Weapons Engineering; Lieutenant, Republic of China Taiwan Navy.

‡Graduate Student, Weapons Engineering; Lieutenant, U.S. Navy.

§Graduate Student, Aeronautical Engineering; Captain, U.S. Army.

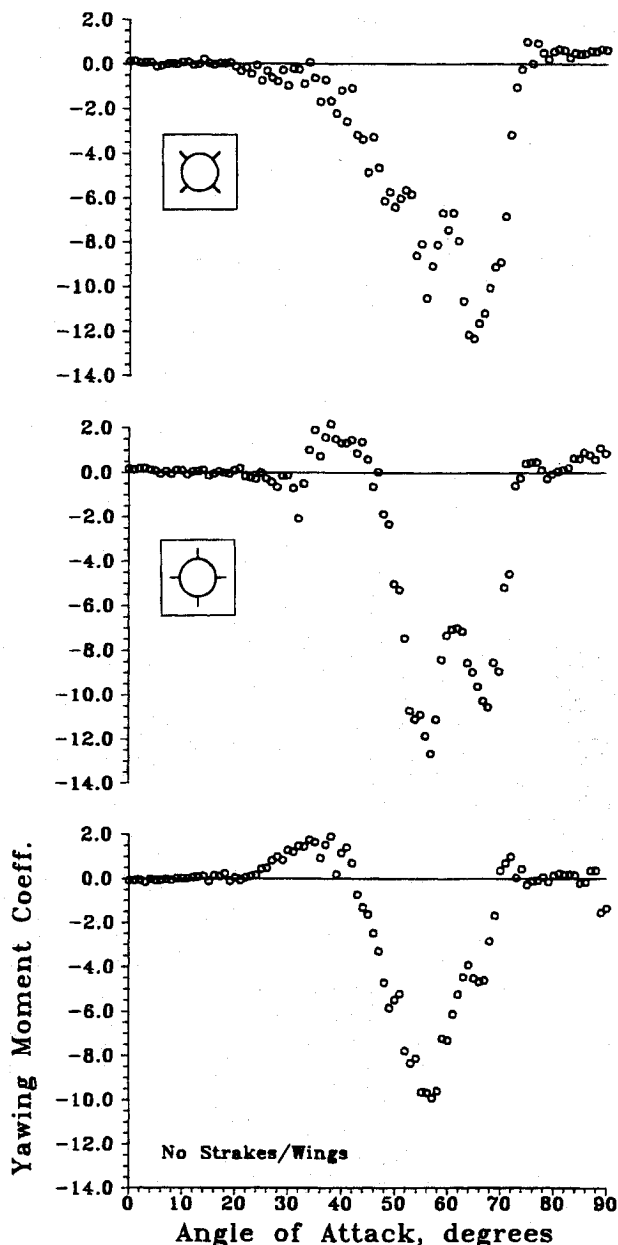


Fig. 2 Yawing moments for missile configurations; Reynolds number = 110,000, Mach number = 0.1.

the formation of asymmetric vortices. The surface-to-air missile modeled possesses long, very low-aspect-ratio cruciform wing-and-strake lifting surfaces, running over half the body length (Fig. 1). A model with a similar wing and tail configuration was tested<sup>1</sup> at a Mach number 0.5 and up to 50 deg angles of attack for roll angles of 0 and 45 deg. A comparison to the body-only case showed a decrease in the maximum induced side force of about 75%. The authors noted that "the out-of-plane forces were largely eliminated by the presence of the strake's [wings]."

### Experimental Program

The model is representative of current ship-based vertically launched surface-to-air missiles. Forces and moments were measured using an internal sting-mounted six-component strain-gauge balance over a range of angles of attack up to 90 deg. Only yawing moments are presented here. The Reynolds number, based on model diameter and freestream velocity, was  $1.1 \times 10^5$ ; the test Mach number was 0.1. The ambient turbulence intensity in the wind tunnel was 0.2%. Moment coefficients were referenced to the body cross-sectional area and body diameter. The moment reference center was at a distance of 0.586 the length of the body measured from the nose.

A nulling five-hole pressure probe was used for the lee flowfield measurements at 50 deg angle of attack. Pressure data were collected in planar survey grids, from which the local velocity magnitude and direction were extracted. Although total pressure plots are also helpful in characterizing the vortex flowfield, only velocity vector data are presented here. See Ref. 6 for a more complete description of the model, test conditions, and results.

Figure 2 shows the yawing moment coefficients for the wingless configuration, the 0-deg wing-roll-angle case, "+", and the 45-deg wing-roll-angle case, "x". Maximum values increase with the addition of the strakes and wings, remaining large between 55 and 70 deg. A change in the sign of the yawing moment at about 45 deg for the wingless and + cases is indicative of the movement of the side force from the afterbody to the forebody; for both cases, the yawing moment changed sign for a constant sign side force (not shown here). The study was performed for a single-nose roll angle, chosen for generating a high maximum side force. In other words, the nose angle was held fixed, while the body was rotated 45 deg. Other roll angles might produce different results. It is clear that a reduction in induced yawing moment with the addition of wings and strakes may not be expected.

Crossplane studies were carried out at an angle of attack of 50 deg. Velocity vectors in the survey plane 11 diameters

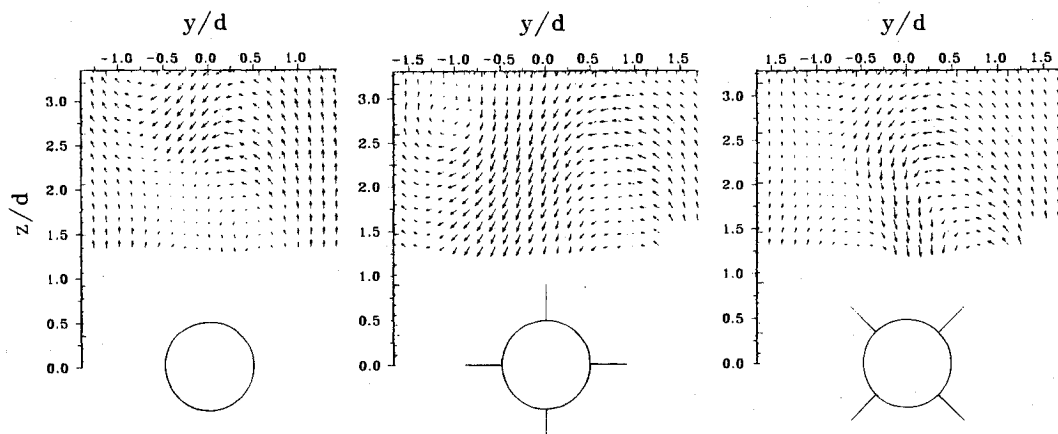


Fig. 3 Cross-plane velocity vectors for missile configurations, 11 diameters aft of nose; angle of attack, 50 deg.

downstream of the missile nose (measured along the body) are shown in Fig. 3 for the three configurations. Survey planes were measured normal to the freestream direction, rather than to the missile axis. The spanwise dimension  $y$  and the vertical distance from the missile centerline  $z$  have been made dimensionless by the model diameter  $d$ . The location of the missile center in the crossplane is accurately plotted, although the missile cross section is not shown as elliptical. Multiple vortices may be expected this far back in the flowfield for the 13-caliber missile. The view in the figure is looking downstream.

In each case, the right vortex is slightly below the survey plane, close to the missile. The left nose-generated vortex has moved up and out of the survey plane for the body-only and  $\times$  configurations. For these configurations, the vectors indicate the formation of a second left vortex below the survey grid, and close in to the centerline. In contrast, the  $+$  configuration shows the left vortex to be clearly within the survey grid, centered at  $y/d = -1.0$  and  $z/d = 2.8$ , with no indication of a second left vortex. The two winged cases show strong inflow toward the missile body. Interestingly, the general crossplane vector field of the  $\times$  case is more similar to that of the body-only than to that of the  $+$  case. Although the lee flowfields are quite different for the two wing-body configurations, the orientation does not significantly influence the effects of the forebody-generated vortices in producing large yawing moments.

### References

- <sup>1</sup>Gregoriou, G., and Knoche, H. G., "High Incidence Aerodynamics of Missiles during Launch Phase," Messerschmitt-Bolkow-Blohm GmbH, Ottobrunn/Munich, Germany, Report UA-523/80, Jan. 1980.
- <sup>2</sup>Keener, E. R., "Flow-Separation Patterns on Symmetric Forebodies," NASA TM-86016, Jan. 1986.
- <sup>3</sup>Ericsson, L. E., and Reding, J. P., "Asymmetric Vortex Shedding from Bodies of Revolution," *Tactical Missile Aerodynamics*, edited by M. J. Hemsch and J. N. Nielsen, Vol. 104, Progress in Astronautics and Aeronautics, AIAA, New York, 1986, pp. 243-296.
- <sup>4</sup>Hunt, B. L., "Asymmetric Vortex Forces and Wakes on Slender Bodies," AIAA Paper 82-1336, Aug. 1982.
- <sup>5</sup>Dunne, A. L., Black, S., Schmidt, G. S., and Lewis, T. L., "VLA Missile Development and High Angle of Attack Behavior," *Proceedings of NEAR Conference on Missile Aerodynamics*, Monterey, CA, 1988, edited by M. R. Mendenhall, D. Nixon, and M. F. E. Dillenius, Nielsen Engineering and Research, Inc., Mountain View, CA, 1988, pp. 13-1-13-68.
- <sup>6</sup>Howard, R. M., Lung, M. H., Viniotis, J. J., Johnson, D. A., and Pinaire, J. A., "Wing Effects on Asymmetric Vortex Formation for a Ship-Launched Missile," AIAA Paper 90-2851, Aug. 1990.

## Nuclear Explosive Propelled Interceptor for Deflecting Objects on Collision Course with Earth

Johndale C. Solem\*  
Los Alamos National Laboratory,  
Los Alamos, New Mexico 87545

### Nomenclature

- $A_p$  = projected area of pusher plate,  $\text{cm}^2$   
 $E$  = energy of impact, erg  
 $g$  = Earth gravitational constant,  $\text{cm} \cdot \text{s}^{-2}$   
 $I_{sp}$  = specific impulse, s

Received March 6, 1992; revision received Sept. 17, 1993; accepted for publication Oct. 2, 1993. Copyright © 1993 by the American Institute of Aeronautics and Astronautics, Inc. All rights reserved.

\*Coordinator for Advanced Concepts, Theoretical Division, Los Alamos National Laboratory, P.O. Box 1663.

- $M_a$  = mass of assailant, gm  
 $M_e$  = mass of crater ejecta, gm  
 $M_f$  = final mass of interceptor, gm  
 $M_i$  = initial mass of interceptor or mass in orbit, gm  
 $m_b$  = mass of nuclear explosive, gm  
 $P$  = impulsive pressure at pusher plate,  $\text{dyne} \cdot \text{cm}^{-2}$   
 $Q$  =  $\ln(M_i/M_f)$  (dimensionless)  
 $\mathcal{R}_i$  = range when assailant is intercepted, cm  
 $\mathcal{R}_l$  = range when interceptor is launched, cm  
 $r$  = distance from nuclear explosive to pusher plate, cm  
 $t_0$  = time when first debris arrives at pusher plate, s  
 $V$  = interceptor velocity,  $\text{cm} \cdot \text{s}^{-1}$   
 $v$  = closing speed of assailant,  $\text{cm} \cdot \text{s}^{-1}$   
 $v_\perp$  = assailant transverse velocity component,  $\text{cm} \cdot \text{s}^{-1}$   
 $Y$  = energy yield of nuclear explosive, erg  
 $\alpha$  = crater constant,  $\text{gm}^{(1-\beta)/2} \cdot \text{cm}^{-\beta} \cdot \text{s}^\beta$   
 $\beta$  = crater exponent, dimensionless  
 $\Delta t$  = time elapsed from launch to intercept, s  
 $\Delta V$  = velocity imparted to interceptor by a single nuclear explosion,  $\text{cm} \cdot \text{s}^{-1}$   
 $\delta$  = energy fraction, dimensionless  
 $\epsilon$  = assailant deflection distance, cm

### Introduction

IN 1992, the House Committee on Science, Space, and Technology mandated a study on the deflection of large space objects that might collide with the Earth.<sup>1</sup> The mandate reflects a heightened concern about the hazards of comets and asteroids ranging in diameter from  $\sim 100$  m, such as the Tunguska object,<sup>2</sup> to several kilometers, such as the Cretaceous-Tertiary Impactor.<sup>3</sup> That our planet is in a continual state of cosmic bombardment has spurred several studies in the past.<sup>4-6</sup>

In a terminal defense scenario, it is generally accepted that a missile must deliver a nuclear explosive to the assailant object in order to deflect it.<sup>7</sup> Preparing such a missile has obvious arms-control implications. This paper shows that assailants could be deflected using an extremely high-specific-impulse interceptor without an explosive warhead. However, nuclear-explosive propulsion will be required to obtain such specific impulse.

### Interceptor Flight and Assailant Deflection

Assuming it is launched from space, the final velocity of an interceptor missile relative to the Earth is given by the rocket equation

$$V = g I_{sp} \ln(M_i/M_f) \quad (1)$$

where  $g \approx 980 \text{ cm} \cdot \text{s}^{-2}$ . In general, the time required to reach this relative velocity will be short compared to the total flight time. The time elapsed from launch to intercept is  $\Delta t = \mathcal{R}_i/(v + V)$ . So the range at which the assailant is intercepted will be  $\mathcal{R}_i = \mathcal{R}_l [1 - v/(v + V)]$ . If the impact gives  $v_\perp$ , then the assailant will miss its target point by a distance

$$\epsilon = \mathcal{R}_l \frac{v_\perp}{v} \left( \frac{V}{v + V} \right) \quad (2)$$

where the effect of the Earth's gravitational field is neglected. To obtain the transverse velocity component, we would use the kinetic energy of the interceptor to blast a crater on the side of the assailant. The momentum of the ejecta would be balanced by the transverse momentum imparted to the assailant. From Glasstone's empirical fits,<sup>8</sup> the mass of material ejected by a large explosion

$$M_e = \alpha^2 E^\beta \quad (3)$$